Excitation of low lying natural parity levels in ^{208}Pb by inelastic electron scattering

J. Heisenberg
University of New Hampshire, Durham, New Hampshire 03824

J. Lichtenstadt
Tel Aviv University, Ramat-Aviv, Tel Aviv, Israel

C. N. Papanicolas
University of Illinois, Urbana, Illinois 61801

J. S. McCarthy
University of Virginia, Charlottesville, Virginia 22901

(Received 16 October 1981)

High resolution electron scattering measurements on ^{208}Pb have been performed at 90° and 160°, which allow the spatial reconstruction of transition charge densities and for the first time, transition current densities. The measurement covering the momentum transfer range of $0.5 < q < 2.6$ fm^{-1} is supplemented by high momentum transfer data from Saclay, extending the data for some of the states up to a momentum transfer of 3.4 fm^{-1}. We report on the first three $J^\pi = 5^-$ states and the first $J^\pi = 7^-$ state. Transition charge densities have been also extracted for the lowest $J^\pi = 2^+$, 4^+, 6^+, and 8^+ states. The densities are compared to a number of theoretical calculations. Transverse electric currents are shown for the 5^- states that indicate a quenching of the magnetization current similar to observations from other states but the absence of quenching in the convection current contribution.

[NUCLEAR REACTIONS ^{208}Pb(e,e') measured cross sections at 90° and 160°, $0.5 \leq q \leq 2.6$ fm^{-1}. Low lying $J^\pi = 2^+$, 4^+, 6^+, 8^+, 5^-, 7^- states analyzed. Transition charge densities and current densities extracted in DWBA.]

I. INTRODUCTION

^{208}Pb is one of the most intensively investigated nuclei, both experimentally and theoretically. Almost any available probe has been used to study this nucleus and numerous nuclear structure calculations complement the experimental work. Since the description of ^{208}Pb as a spherical and doubly-closed shell nucleus is rather good, various aspects of its nuclear structure can be isolated to a good degree and studied independently of each other. In this paper, we will present and discuss results obtained from the electroexcitation of several low-lying states. These results pose very strong constraints to any nuclear structure calculation attempting to describe this nucleus.

The well understood electromagnetic interaction makes electrons an exceptionally precise probe in experimental nuclear structure studies. The electromagnetic probe, being relatively weak, allows the separation of the reaction mechanism from the nuclear structure under study, thus making it probably the cleanest probe available. It allows the determination of the nuclear transition charge and current densities from which conclusions about nuclear structure in general and the residual interaction in particular can be made.

The ^{208}Pb ground state charge density has been investigated repeatedly in the past. The (e,e) experiment at Saclay[1] extended the electron scattering data up to the momentum transfer of 3.5 fm^{-1}. Together with the very accurate low momentum transfer data and the muonic x-ray transition energies, it enabled a very precise determination of the ground state charge distribution.[2] The results give valuable information on the quality of Hartree-Fock calculations for the nuclear ground state.[3,4] Similarly, the investigation of excited states of the nu-

cleus sheds light on many nuclear structure questions such as the nature of the effective residual interaction, its strength, and more.

In the past, the lack of high energy, high intensity electron beams, together with high resolution detection systems, has limited the inelastic electron scattering experiments to the study of low-lying collective states that are strongly excited and well resolved. Such previous studies include the investigation of the lowest 3^- level at 2.615,[5] the 5^- levels at 3.198 and 3.709 MeV (Refs. 6 and 7), as well as the positive parity band[8] 2^+, 4^+, 6^+, 8^+, and 10^+.

The new generation of high resolution electron scattering facilities (like those at the Bates Linear Accelerator and the Saclay accelerator) eliminate these shortcomings making now possible the investigation of excited states to weaker excitations of single-particle hole character such as the high multipolarity transitions where the high resolution, high intensity, and high incident energy are preconditional. The inclusion of the recent high momentum transfer data from Saclay[5,9] in the analysis of the 3^- and 5^- levels allowed the determination of the transition charge density for the $J^\pi = 3^-$, 5^- states with an accuracy equaling that of the ground state charge distribution. With these facilities, it is possible to study aspects that have not been accessible so far, such as weak states or the magnitude of the transverse form factors. We have already reported on the identification of high spin states in ^{208}Pb,[10,11] and we present in this paper, the results from the low-lying states below 4.61 MeV that are indicated in Fig. 1. These results not only allow a more precise determination of the transition charge density distributions to the various levels involved, but they also give, for the first time, a measure of the transverse form factors for several of these states.

II. EXPERIMENTAL PROCEDURE AND DATA REDUCTION

The experiment was done using the MIT-Bates electron scattering facility. The accelerator and the spectrometer, with its focal plane detection system, have been described elsewhere.[12,13] Hence, only a brief summary of the facts relevant to our experiment will be given.

The Bates linac can provide an electron beam with an incident energy up to 400 MeV. The beam pulse widths are typically 10 μsec with repetition rates of a few hundred pulses per second. Employing the dispersion matching technique in the beam transport between the accelerator and the spectrometer, the entire beam of $\Delta p/p = 0.2\%$ can be utilized obtaining still high resolution spectra in the energy loss, of $\Delta p/p \leq 2\times 10^{-4}$ at the focal plane. Thus, the combination of high incident energy and current electron beams with high resolution detection capability, essential in this experiment, could be achieved. Currents up to 45 μA were used in this experiment.

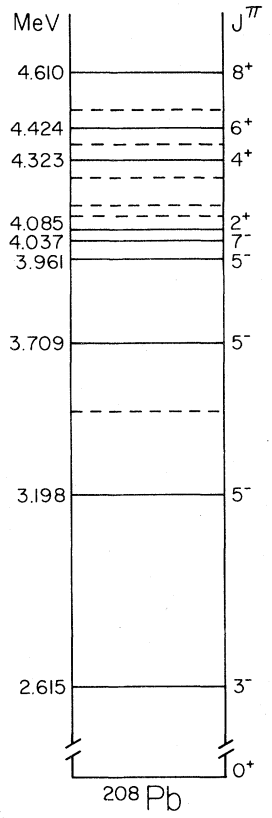

FIG. 1. Levels in ^{208}Pb observed in this experiment. Levels indicated by a solid line are discussed in this paper.

The experiment was done with incident beam energies from 50 to 335 MeV, detecting the scattered electrons at 90° or at 160°. Thus, the momentum transfer region $0.3 < q < 2.6$ fm^{-1} was probed at both angles.

The electron detection system is located at the spectrometer focal plane. It consists of a transverse (to the electron track) multiwire proportional chamber and a vertical drift chamber, which read the transverse position and the momentum coordinate of the detected electron, respectively. Two Cerenkov counters (located underneath the chambers) provide the fiducial start to the readout scheme. A coincidence requirement between the Cerenkov counters helps background rejection im-

proving the signal to noise ratio of the measured peaks. The wires in the vertical drift chamber are arranged in three delay lines. The arrival times of the signals from the firing wires to both sides of each delay line, as well as those from the transverse array (relative to the Cerenkov fiducial), are measured by an 8-channel time-to-digital converter (TDC), and used to compute the position and the angle of incidence for the electron track. The momentum acceptance of the detection system is 6%. Several spectra were taken in the low-energy runs, with different magnetic field settings to obtain the higher excitation regions up to 7 MeV.

The incident electron energies and the spectrometer's linear and quadratic dispersion parameters were determined by measuring the recoil energy differences between the elastic peaks of ^{9}Be, ^{16}O, ^{27}Al, and ^{208}Pb together with peak positions of excited states in these nuclei with well-known excitation energies. The spectrometer's magnetic field was measured with a nuclear magnetic resonance (NMR) probe. The resulting uncertainty in the incident energy was generally less than 0.2%.

The targets used were ^{208}Pb foils 99% enriched of 60, 30, and 10 mg/cm^2 thickness. At 90°, the 30 mg/cm^2 target was used for energies below 275 MeV and the 60 mg/cm^2 target above that energy, both in transmission mode. The 10 mg/cm^2 target was used in reflection mode in the 160° runs.

Owing to a relatively low temperature melting point of lead, the maximum average current, which could be used at the Bates linac without target cooling arrangements, was about 10 μA. At high energy incident beams and particularly at backward angles where the counting rate is rather low, target cooling techniques were employed to allow higher incident beam currents. Two methods were adopted. In the first, hydrogen gas was blown against both sides of the target. The gas in the chamber was circulated to maintain a gas pressure of about 1 Torr. Alternatively, the targets were mounted on circular frames, which were spun at the rate of a few revolutions per second, while the beam was hitting the target off center. Both arrangements allowed running with incident beam currents as high as 45 μA.

The beam charge was monitored by nonintercepting ferrite core torroids,[14] which were tested to have an accuracy better than 10^{-3}. The solid angle utilized was around 3 msr. To avoid inefficiencies near the edges of the detection system, the momentum acceptance was limited to 5% only. The relative wire-to-wire efficiencies were tested by measuring a smooth spectrum in the region of the quasielastic peak and were shown to be uniform to within 5%. To check for slow variations in efficiency across the detector system, the elastic peak of ^{208}Pb was measured at several locations along the focal plane and was found to be uniform to within 1.5%.

The 90° data and the lower energy 160° data were normalized to the elastic ^{208}Pb cross section calculated with a phase shift code from the best fit charge distribution that was fitted to all available (e,e) and muonic x-ray transition data.[2] At 160°, we took absolute measurements, since the elastic peak was too weak to determine an adequate normalization. The normalizations for incident energies below 180 MeV indicated agreement to within 5%.

A total of 19 spectra were taken at 90°, and 14 spectra at 160°. Typical spectra with an energy resolution of about 30 keV, taken at both angles, are shown in Fig. 2. To extract the cross section from the raw data, a line-shape, fitting program was used in which an asymmetric Gaussian shape is folded with the effects of Landau straggling, bremsstrahlung, and Schwinger radiation following the method of Bergstrom.[15] In general, the peak shapes were locked to those of strong excitations. The excitation energies of the fitted levels were allowed to vary only when the peaks were well defined and resolved. Otherwise, they were locked to the known excitation energies measured by the (p,p') experiment of Wagner *et al*.[16]

III. ELECTRON SCATTERING ANALYSIS

The electron scattering cross section is given in Born plane wave approximation by:

$$\frac{d\sigma}{d\Omega}=\sigma_M\left[\sum_{\lambda\geq 0}|F_2^c(q)|^2+\left[\tfrac{1}{2}+\mathrm{tg}^2\frac{\vartheta}{2}\right]\sum_{\lambda\geq 1}(|F_\lambda^E(q)|^2+|F_\lambda^M(q)|^2)\right] \tag{1}$$

with

$$\sigma_M=\frac{\pi\alpha^2}{E_i^2\sin^4\frac{\vartheta}{2}}\cos^2\frac{\vartheta}{2}\left[1+\frac{2E_f}{M_T}\sin^2\frac{\vartheta}{2}\right]^{-1} \tag{2}$$

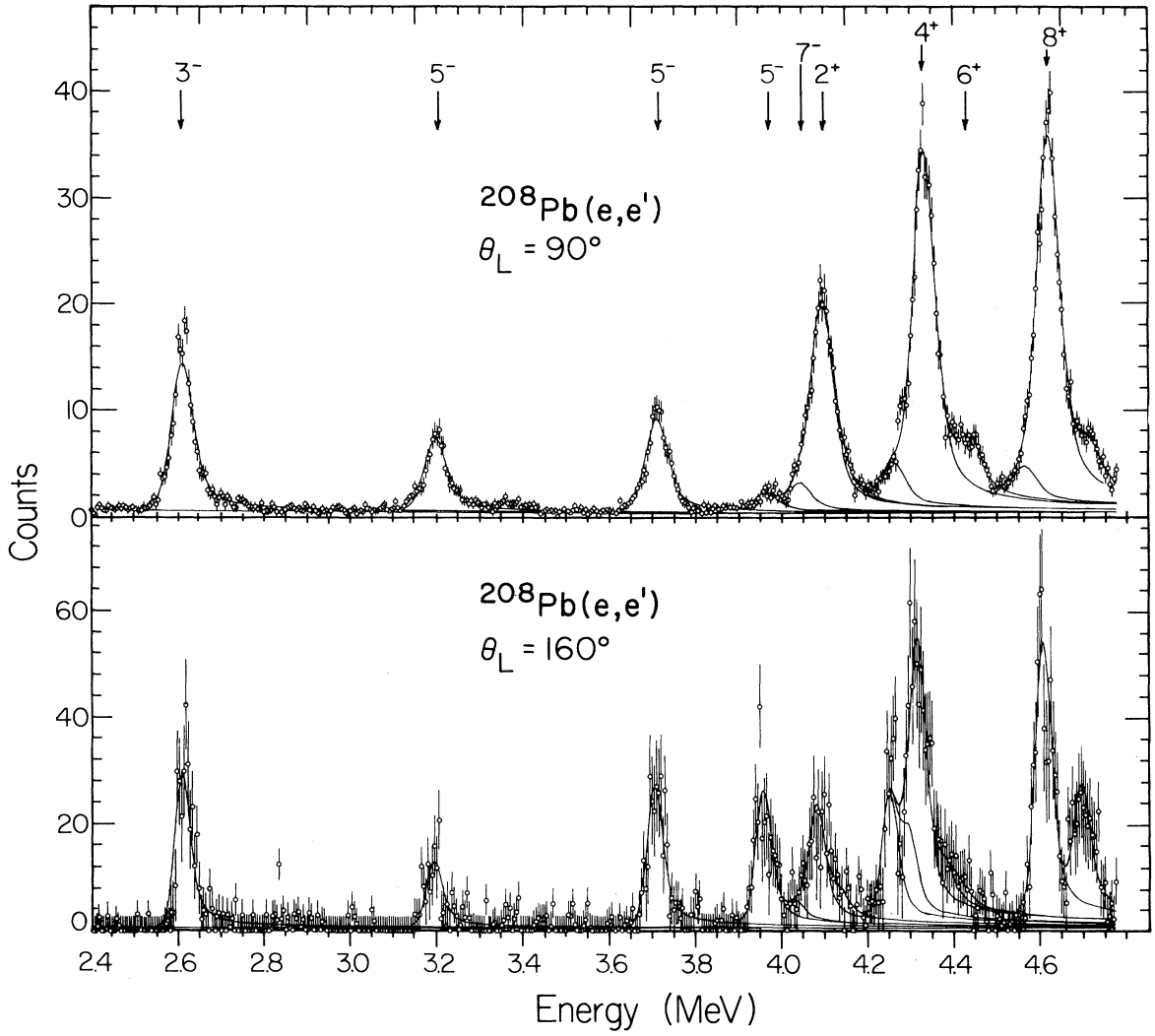

FIG. 2. Spectra of scattered electrons taken at 202 MeV incident energy and 90° shown on the upper part, and 140 MeV incident energy and 160° in the lower part. The two spectra match approximately in momentum transfer.

and the momentum transfer q given by

$$q=2\sqrt{E_i E_f}\sin\frac{\vartheta}{2}\ . \tag{3}$$

For plotting purposes as well as for the purpose of recalculation (as discussed below), we use the quantity

$$q_{\text{eff}}=q\left[1+\frac{4}{3}\frac{Z\alpha}{E_i R_{\text{rms}}}\right]\ . \tag{4}$$

The form factors can be written as Fourier Bessel (FB) transforms of the nuclear one body transition densities

$$F_\lambda^c(q)=\frac{\hat{J}_f}{\hat{J}_i}\int_0^\infty \rho_\lambda(r)j_\lambda(qr)r^2dr\ , \tag{5}$$

$$F_\lambda^E(q)=\frac{\hat{J}_f}{\hat{J}_i\hat{\lambda}}\left[\sqrt{\lambda+1}\int_0^\infty J_{\lambda,\lambda-1}(r)j_{\lambda-1}(qr)r^2dr+\sqrt{\lambda}\int_0^\infty J_{\lambda,\lambda+1}(r)j_{\lambda+1}(qr)r^2dr\right], \tag{6}$$

$$F_\lambda^M(q)=\frac{\hat{J}_f}{\hat{J}_i}\int_0^\infty J_{\lambda,\lambda}(r)j_\lambda(qr)r^2dr\ . \tag{7}$$

For spin 0 nuclei such as ^{208}Pb, only one multipolarity contributes in the sum of Eq. (1). The magnetic form factor F^M contributes only in the excitation of the unnatural parity states, which are not being discussed in this paper, while the longitudinal and the transverse electric form factors contribute only to the excitation of the natural parity states. In the case of a natural parity transition, the three nuclear transition densities $\rho_\lambda(r)$, $J_{\lambda,\lambda-1}(r)$, and $J_{\lambda,\lambda+1}(r)$ are connected through the continuity equation:

$$\hat{\lambda}\frac{\hbar\omega}{\hbar c}\rho_\lambda(r)=\sqrt{\lambda}\left[\frac{\lambda-1}{r}-\frac{d}{dr}\right]J_{\lambda,\lambda-1}(r)-\sqrt{\lambda+1}\left[\frac{\lambda+2}{r}+\frac{d}{dr}\right]J_{\lambda,\lambda+1}(r) \tag{8}$$

Thus the cross section is completely specified through any combination of only two of these radial quantities. While it is more convenient to calculate the cross sections in the distorted wave Born approximation (DWBA) from the two currents $J_{\lambda,\lambda-1}(r)$ and $J_{\lambda,\lambda+1}(r)$ (Ref. 17), we believe that within nuclear models where the continuity equation is not strictly satisfied $\rho_\lambda(r)$ can be calculated more reliably than the other two. We, therefore, choose to represent our data through the densities $\rho_\lambda(r)$ and $J_{\lambda,\lambda+1}(r)$, which completely specify the measured cross section.

The transition between the various representations mentioned can be easily performed within the Fourier Bessel expansion. In this method, it is assumed that outside the nucleus all transition densities decrease rapidly with increasing radius so that beyond a certain radius R_c, all densities can be set equal to zero. For $r<R_c$, the densities can be expanded in the following form[17]:

$$\rho_\lambda(r)=\sum_\mu A_\mu q_\mu^{\lambda-1}j_\lambda(q_\mu^{\lambda-1}r)\ , \tag{9}$$

$$J_{\lambda,\lambda+1}(r)=\sum_\mu B_\mu j_{\lambda+1}(q_\mu^\lambda r)\ , \tag{10}$$

$$J_{\lambda,\lambda-1}(r)=-\frac{1}{\sqrt{\lambda}}\left[\hat{\lambda}\frac{\hbar\omega}{\hbar c}\sum_\mu A_\mu j_{\lambda-1}(q_\mu^{\lambda-1}r)+\sqrt{\lambda+1}\sum_\mu B_\mu j_{\lambda-1}(q_\mu^\lambda r)\right], \tag{11}$$

where $q_\nu^\lambda R$ is the νth zero of the Bessel function of order λ. This parametrization always satisfies the continuity equation. In the plane wave Born approximation, the divergenceless current $J^{\rm tr}$, as given by the coefficients B_ν, would lead to a completely transverse cross section. We call the remaining part of the current term $J_{\lambda,\lambda-1}$ the irrotational and incompressible current $J^{\rm ir}(r)$. It is uniquely tied to the transition charge $\rho_\lambda(r)$ through the continuity equation. We should stress, though, that some small transverse cross section is already produced by the irrotational and incompressible current $J^{\rm ir}(r)$. The justification for using $q_\nu^{\lambda-1}$ instead of q_ν^λ in Eq. (9) is given in Ref. 17. The division of the currents into one term describing irrotational and incompressible flow (terms depending on A_ν) and a second term accounting for a divergenceless current (terms depending on B_ν) is somewhat arbitrary but without loss of generality. We chose this particular division for two reasons: (1) The coefficients A_ν can be determined solely from the transition charge density $\rho_\lambda(r)$ while the coefficients B_ν can be determined solely from the transition current density $J_{\lambda,\lambda+1}(r)$, and (2) experiments support the idea that the dynamics of collective motion behave like irrotational and incompressible flow. Thus, the magnitude of the divergenceless terms seems to be an indication of the collectivity of a transition.

Most electron scattering experiments in the past have been analyzed assuming the modified Tassie model, i.e., assuming that the coefficients B_ν are negligibly small. In this form, the modified Tassie model is just a restriction to irrotational, incompressible flow. In the most general analysis in which the densities are being reconstructed from the experiment, both sets of coefficients A_ν and B_ν are fit-

ted by a least-squares method to the experimental data that must cover the same momentum transfer region both in forward and in backward direction. In the cases discussed in this paper, we deal mostly with collective states for which the description as an incompressible and irrotational flow is a fairly good description of the dynamics. Consequently, the information on the small current density $J^{\rm tr}(r)$ from this experiment is rather limited. Thus, it seemed more appropriate to fit the data using a more restrictive model as will be discussed in more detail below.

IV. TRANSITION DENSITIES IN THE MICROSCOPIC DESCRIPTION OF EXCITED STATES

The nuclear structure of the low-lying levels in ^{208}Pb is usually described in terms of the random phase approximation (RPA) assuming that the effects of ground state correlations can be adequately accounted for by RPA correlations. The collective states are described through the creation of a phonon from the nuclear ground state using the phonon creation operator

$$Q^\dagger=\sum_{\rm ph} X_{\rm ph}(a_p^\dagger a_h)-Y_{\rm ph}(a_h^\dagger a_p)\ . \tag{12}$$

Within this context, the transition densities are given as

$$\rho_\lambda(r)=\frac{\hat\lambda}{\hat J_f}\sum_{\rm ph}(X_{\rm ph}+Y_{\rm ph})\rho_\lambda^{\rm ph}(r)\ ,$$

$$J_{\lambda,\lambda'}(r)=\frac{\hat\lambda}{\hat J_f}\sum_{\rm ph}(X_{\rm ph}-Y_{\rm ph})\times[J^{c,{\rm ph}}_{\lambda,\lambda'}(r)+J^{M,{\rm ph}}_{\lambda,\lambda'}(r)]\ , \tag{13}$$

where the single ph densities are given by Lee[18] in terms of the radial part u of the wave functions, and its derivatives u'

$$\rho_\lambda^{\rm ph}(r)=S^\lambda_{\rm ph}u_p(r)u_h(r)\ ,$$

$$S^\lambda_{\rm ph}=(-1)^{j_h-1/2}\frac{\hat j_p\hat j_h}{\sqrt{4\pi}}\begin{pmatrix} j_p & j_h & \lambda\\ \frac12 & \frac12 & 0\end{pmatrix}\ , \tag{14}$$

$$J^{c,{\rm ph}}_{\lambda,\lambda+1}(r)=\frac{\hbar c}{2mc^2}S^\lambda_{\rm ph}\frac{1}{\sqrt{\lambda+1}\hat\lambda}\left\{(\lambda+1)[u_p(r)u_h'(r)-u_h(r)u_p'(r)]+[l_p(l_p+1)-l_h(l_h+1)]\frac{u_p(r)u_h(r)}{r}\right\}\ , \tag{15}$$

$$J^{c,{\rm ph}}_{\lambda,\lambda-1}(r)=-\frac{\hbar c}{2mc^2}S^\lambda_{\rm ph}\frac{1}{\sqrt{\lambda}\hat\lambda}\left\{\lambda[u_p(r)u_h'(r)-u_h(r)u_p'(r)]-[l_p(l_p+1)-l_h(l_h+1)]\frac{u_p(r)u_h(r)}{r}\right\}\ , \tag{16}$$

$$J^{M,{\rm ph}}_{\lambda,\lambda+1}(r)=\mu\frac{\hbar c}{2mc^2}S^\lambda_{\rm ph}\frac{1}{\sqrt{\lambda+1}\hat\lambda}(\chi_p-\chi_h)\left[\frac{d}{dr}-\frac{\lambda}{r}\right]u_p(r)u_h(r)\ , \tag{17}$$

$$J^{M,{\rm ph}}_{\lambda,\lambda-1}(r)=-\mu\frac{\hbar c}{2mc^2}S^\lambda_{\rm ph}\frac{1}{\sqrt{\lambda}\hat\lambda}(\chi_p-\chi_h)\left[\frac{d}{dr}+\frac{\lambda+1}{r}\right]u_p(r)u_h(r)\ , \tag{18}$$

with $\chi=(l-j)(2j+1)$.

Comparisons of the transition charge density with theoretical calculations show that the main features that lead to collectivity are understood. However, very little is known about the currents in nuclei. Tassie's description for collective motion as an irrotational and incompressible flow[19] leads to currents in which the contributions from $J^{\rm tr}(r)$ vanish. Thus, within this context, the absence of these currents may be taken as a measure of collectivity. In microscopic models (such as the RPA), the current terms $J^{\rm tr}(r)$ are nonzero but are usually strongly reduced compared to single particle values, depending on the collectivity of the level. Thus, again, the magnitude of $J^{\rm tr}(r)$ gives some indication of the collectivity of a level.

In addition to the core polarization through the residual interaction, which is described adequately by the RPA, the currents are reduced through ground-state correlations. These correlations affect

positive and negative parity states in different ways. While the main effect of these correlations is to enhance the transition charge density and produce destructive interference in the currents, it also provides partial shell occupations, thereby allowing the generation of considerable strength in the positive parity states from the pair breakup modes $(j)_{0^+}{}^2 \rightarrow (j)_{\lambda^+}{}^2$ usually not contained in the RPA treatment. In a microscopic single particle model, the currents of these modes vanish exactly. Thus, strong contributions in the excitation of the positive parity states from such modes will lead to particularly small transverse form factors. For negative parity states, the reduction has to come from random phases in the many small nonzero contributions.

In addition, currents are affected by subnucleonic degrees of freedom, which usually are lumped into exchange currents. The magnitude of these corrections is not yet well established. There is, however, no experimental way to separate these contributions from the others.

Since the size of the transverse current $J^{\rm tr}(r)$ is an interesting quantity to measure, we will discuss the sensitivity of experiments. As pointed out above, there is always some transverse strength connected with the irrotational, incompressible flow term. Thus, the limit of sensitivity in an experiment is achieved at a scattering angle where the longitudinal scattering is small compared to the always present irrotational, incompressible flow term. This irrotational, incompressible flow term is generally quite small and for a state such as the 3^- level even at 179° and for $q > 1.0$ fm^{-1}, its transverse part accounts for less than 25% of the total cross section. As can be seen from this estimate, considerable sensitivity can still be gained through a 180° scattering experiment. On the other hand, if the backward measurement is considered merely for the purpose of correcting the 90° data for any transverse contributions, a scattering angle of 160° quite suffices.

It should be noted that for levels that have substantial $J^{\rm tr}$ contributions (such as the 7^- state at 4.037 MeV), the maximum sensitivity is obtained at considerably smaller scattering angles. For those states, the maximum sensitivity is already achieved in the comparison between 90° and 160° data.

V. RESULTS FROM THE POSITIVE PARITY STATES

The data that were included in the analysis with our data are those of Ziegler and Peterson.[20] The data of the Mainz group[8] were taken with insufficient resolution to separate the 7^- level at 4.037 MeV, the 5^- level at 4.160 MeV, or the group of levels at 4.256 MeV. For that reason, these data disagree with our data mostly in the diffraction minima, and we refrained from including them in our analysis. For all the data, 5% of the cross section has been added in quadrature to the error in order to account for errors due to normalization or determination of the incident energy.

All the positive parity transitions discussed here are dominantly longitudinal. The data can be used to reconstruct the transition charge densities $\rho_\lambda(r)$. For this purpose, the transition charge density is expanded within a cutoff radius of 12 fm. The tail of the density (beyond a radius of 8.2 fm) has been biased through a χ^2 criterion to follow an analytic shape of $r\exp(-\alpha r)$, where α is also fitted to the data. The higher Fourier-Bessel coefficients not determined by the data were obtained assuming that the form factor drops rapidly with increasing momentum transfer, and assigning an uncertainty given by an exponential upper limit as described in Ref. 17.

A. The 2^+ state at 4.085 MeV

For this state, the data do not extend up to the same momentum transfer as the other states. The reason is the 7^- level at 4.037 MeV that is separated by only 50 keV, but has at high momentum transfer a much larger cross section than the 2^+ level. Thus, at large momentum transfer, the accuracy of our data is less than that of the other states. The data cover the momentum transfer range of $0.4 > q > 2.6$ fm^{-1}. The experiment determines up to $N=9$ of the Fourier Bessel expansion coefficients, fitting both the 90° and the 160° simultaneously. This analysis differs from the analysis presented in Ref. 17 only by the inclusion of several additional data points and by the larger cutoff radius R_c.

The data from the Bates accelerator allow a check on the magnitude of the transverse current by comparing the fit dominated by the forward scattering data to those taken at 160°. This comparison (shown in Fig. 3) demonstrates the absence of transverse currents to a level where contributions at 160° are less than 10% of the longitudinal form factors. Thus, at 90°, contributions from the transverse form factor are negligible.

A transverse form factor smaller than this level is already predicted by RPA calculations. Thus, our

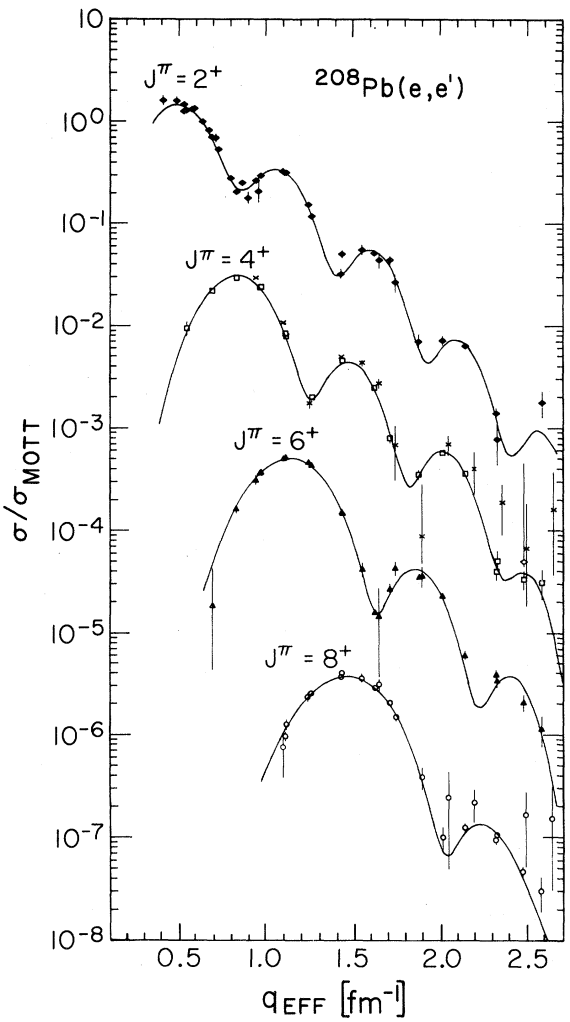

FIG. 3. Cross section for the even spin natural parity states in ^{208}Pb divided by (the cross section for a unit-point charge). Data and best fit for the 4^+ level are scaled down a factor of 0.03, for the 6^+ level a factor of 0.001, and for the 8^+ level a factor of 0.000 03.

data do not have enough sensitivity to allow a measure of ground-state correlations. It is suggested that such experiments be done at 180° where the contributions from the irrotational, incompressible part are considerably smaller.

B. The 4^+ state at 4.323 MeV

Combining the data from 90° to 160° in one fit and neglecting the transverse current J^{tr}, gave unsatisfactory fits with much larger χ^2 than in fitting the 90° or the 160° data separately. This indicates the presence of transverse cross sections, which could either come from an unresolved level or from a real transverse current in this transition. The closest level seen in (p,p') is more than 25 keV separated from this state. Since the resolution in this experiment was typically 30 keV, contributions from this level cannot be excluded even though they seem unlikely.

Because of the small effect, it was impossible to develop a reasonable model for these transverse contributions. For that reason, we have fitted only the forward scattering data where the effects from the transverse components should be considerably smaller than the quoted error bars. The data determine up to $N=8$ coefficients, in the FB expansion.

C. The 6^+ state at 4.424 MeV

The data from the 6^+ state were handled in the same way as for the 2^+ state, since there was no indication for any transverse current in this transition. The data determine up to $N=7$ coefficients, in the FB expansion.

D. The 8^+ state at 4.610 MeV

The data from the 8^+ state again indicate the presence of a small transverse current. This is not surprising since our measurements on 10^+ states[11] show a very strong transverse current that can be described by quenched single particle currents with a quenching factor of 0.65. The currents observed in this 8^+ state are considerably weaker, and we used our data mainly to correct the 90° data for any transverse contributions. This was done assuming quenched currents from the proton component, $\pi(1h_{9/2},\ 1h_{11/2}^{-1})$, the quite dominant neutron $\nu(1j_{15/2},\ 3_{p1/2}^{-1})$, and the neutron $\nu(1i_{11/2},\ 1i_{13/2}^{-1})$ component, which mostly cancels the current contributions from the proton configuration.

In all cases of the positive parity states, it was sensible because of the smallness of the transverse current to recalculate the data to the maximum incident energy. These recalculated data are defined as

$$\left[\frac{d\sigma}{d\Omega}\right]_R = \left[\frac{d\sigma}{d\Omega}\right]_{\text{exp}} \frac{d\sigma(E_{\max},q_{\text{eff}})\text{DWBA}}{d\sigma(E_{\text{exp}},q_{\text{eff}})\text{DWBA}} . \tag{19}$$

These recalculated data are shown together with the best fit in Fig. 3. The fact that for the 2^+ and

the 6^+ level the 160° data show no significant deviation from the combined fit, indicates the absence of the transverse currents to the limit of our experiment. For the 8^+ level, the χ^2 of 1.1/deg of freedom for the 160° data indicates that our iterative procedure corrects properly for any transverse contributions.

The resulting transition charge densities are displayed in Fig. 4, where they are also compared to theoretical predictions from various RPA calculations.[21–23] Their FB expansion coefficients are given in Table I.

VI. RESULTS FROM THE NEGATIVE PARITY STATES

A. The 3^- level at 2.615 MeV

The collective octupole vibration at 2.615 MeV has been subject to several investigations,[24,25] which have been recently summarized by Goutte *et al.*[5] Figure 5 shows our data taken at 160° in comparison to the fit done to the forward scattering data and assuming the absence of $J^{tr}(r)$. This comparison shows that the 160° data are consistent with the absence of $J^{tr}(r)$. In all cases, we use the transition density as extracted from the forward scattering data and presented in Ref. 5. The prediction using $J^{tr}(r)=0$ is hardly distinguishable from the prediction with $J^{tr}(r)$ as given by the RPA from Heisenberg and Krewald.[23] It shows that there is little sensitivity to the exact shape of $J^{tr}(r)$ in our data. It should be pointed out, though, that this is just a consequence of the smallness of $J^{tr}(r)$. As pointed out above, considerable sensitivity would be gained through measurements at 180°.

B. The 5^- levels at 3.198, 3.709, and 3.961 MeV

The negative parity states with spins $J>3$ behave quite differently. Most levels discussed so far show negligible or very small contributions from the current term $J^{tr}(r)$. This is not the case for the 5^- levels in ^{208}Pb, which show substantial transverse cross sections. These transverse currents have been ignored in previous analyses.[6,7] The origin of these transverse currents stems from the microscopic structure of these levels. They can be viewed as a remnant from dominant ph configurations, an interpretation that is consistent with the stripping reaction result,[26] showing for instance, substantial strength of the $\nu(2g_{9/2}\ 3p_{1/2}{}^{-1})$ neutron component in the 3.198 MeV level.

This is essentially reproduced by the RPA giving an amplitude of 0.874 for the $\nu(2g_{9/2},\ 3p_{1/2}{}^{-1})$ component. The RPA result also agrees with the 4% admixture from the proton $\pi(1h_{9/2},\ 3s_{1/2}{}^{-1})$

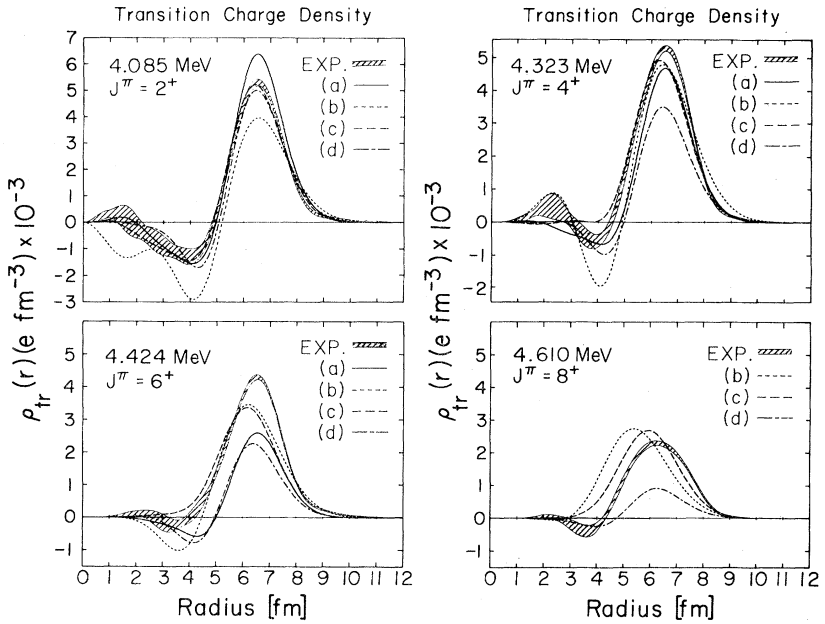

FIG. 4. Transition charge densities for the even spin natural parity states in ^{208}Pb. The theoretical curves are from: (a) Bertsch and Tsai (Ref. 21), (b) Knüpfer and Huber (Ref. 22), (c) Gogny and Dechargé (Refs. 4 and 35), and (d) Heisenberg and Krewald (Ref. 23).

TABLE I. Fourier Bessel coefficients that give the experimental transition charge densities in $10^{-3}\,e/\mathrm{fm}^3$ using a cutoff radius of 12 fm. The absence of errors indicates that the fit was not done in the FBE.

	$2^+(4.085)$	$4^+(4.323)$	$6^+(4.424)$	$8^+(4.610)$
N				
1	8.716±0.453	7.192±0.605	4.728±0.657	1.775±0.741
2	10.881±1.268	14.258±1.396	11.222±1.440	5.540±1.560
3	−4.687±0.173	5.170±0.298	8.660±0.625	6.373±0.810
4	−8.901±0.335	−6.661±0.345	−0.851±0.167	2.250±0.280
5	2.523±0.226	−3.473±0.191	−3.994±0.291	−1.104±0.156
6	4.786±0.204	3.018±0.180	−0.094±0.075	−0.957±0.133
7	−1.476±0.170	1.415±0.125	1.237±0.118	−0.436±0.217
8	−1.518±0.123	−0.672±0.133	−0.341±0.209	−0.431±0.263
9	0.884±0.244	0.327±0.337	−0.321±0.298	0.016±0.246
10	0.302±0.396	0.287±0.310	0.377±0.188	0.230±0.133
11	−0.143±0.292	−0.321±0.242	0.094±0.188	0.031±0.181
12	0.190±0.313	0.064±0.227	−0.033±0.185	0.031±0.128
13	−0.048±0.259	0.116±0.179	0.092±0.086	0.060±0.060
14	−0.040±0.171	−0.080±0.135	0.028±0.080	0.004±0.099
15	0.051±0.122	−0.030±0.096	−0.043±0.056	−0.002±0.066
$B(E\lambda)$	0.318 e^2b^2 ±5%	0.155 e^2b^4 ±7%	0.0665 e^2b^6 ±10%	0.0054 e^2b^8 ±17%

	$5^-(3.198)$	$5^-(3.709)$	$5^-(3.961)$	$7^-(4.037)$
N				
1	3.709±0.218	2.804±0.180	−0.602	0.659
2	7.470±0.491	5.639±0.409	−1.412	1.800
3	3.600±0.198	2.170±0.135	−1.059	1.726
4	−1.874±0.100	−2.646±0.142	−0.807	0.155
5	−0.794±0.054	−1.583±0.093	−1.575	−0.771
6	1.832±0.092	1.185±0.068	−1.267	0.003
7	0.981±0.055	1.099±0.058	0.091	0.753
8	−0.184±0.046	0.435±0.054	0.564	0.383
9	−0.077±0.070	0.307±0.053	0.194	−0.105
10	0.003±0.067	0.089±0.045	−0.032	−0.043
11	−0.003±0.075	0.041±0.048	−0.012	0.100
12	0.067±0.038	0.078±0.022	0.006	0.023
13	−0.004±0.053	0.020±0.028	−0.002	−0.017
14	0.004±0.035	0.017±0.019	−0.001	0.018
15	0.018±0.022	0.022±0.014	0.002	0.017
$B(E\lambda)$	0.0447 e^2b^5 ±6.8%	0.0241 e^2b^5 ±7.5%	0.0008 e^2b^5	0.0010 e^2b^7

component, as measured by McClatchie *et al.*[27]

In the ^{209}Bi $(d,{}^3\mathrm{He})^{208}$Pb reaction,[27] the strength from the proton $\pi(1h_{9/2}, 3s_{1/2}{}^{-1})$ component has been observed mainly in the 3.709 MeV and in the 3.961 MeV states. These two states comprise in lowest order two orthogonal mixtures of the neutron $\nu(2g_{9/2}\ 2f_{5/2}{}^{-1})$ and the proton $\pi(1h_{9/2}, 3s_{1/2}{}^{-1})$ components. The transition charge scattering for these two configurations is produced mainly by the proton component and by all the small amplitudes that couple to the strong neutron configuration. Thus, they follow in phase the neutron configuration and may be referred to as the induced charge. In the 3.709 MeV state this induced

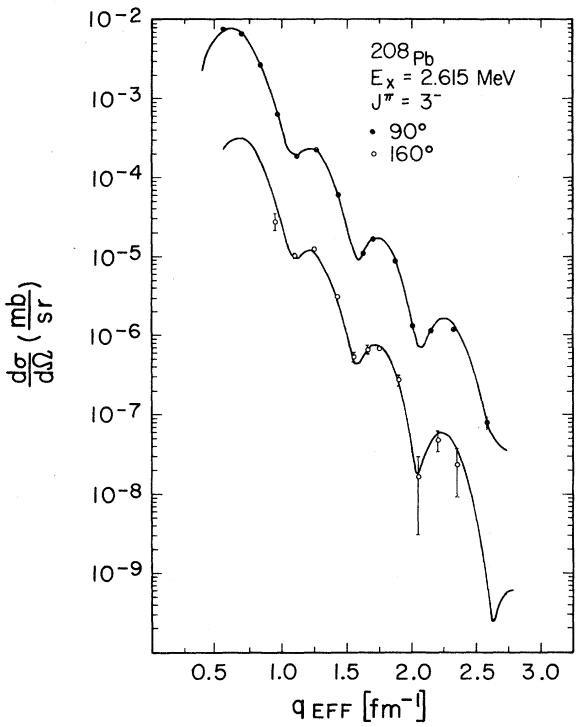

FIG. 5. Cross sections for the 3^- level at 2.615 MeV measured at 160° and compared to the best fit of Ref. 5 assuming the absence of any transverse current.

charge adds constructively at the nuclear surface with the proton component while they add destructively in the 3.961 MeV state. This leads to a drastically different behavior of the forward electron scattering cross sections of these two states. In the 3.961 MeV state, the first diffraction maximum has almost disappeared. This cancellation seizes at higher momentum transfer because of the strongly different q dependences of the form factor for the proton configuration and that for the induced charge. In coordinate space, this can be described as a cancellation or strong reduction of the outer node in the transition charge from the proton configuration by the induced charge. Since the induced charge is mostly surface peaked,[28] no cancellation of the interior node takes place. Thus, the transition charge distribution of the 3.961 MeV state is located in the interior of the nucleus in contrast to the transition charge of the two lower 5^- states.

The transverse currents for all the 5^- states were fitted employing a microscopic model allowing for contributions from all the ph configurations listed in the wave function of Heusler and Brentano.[29] The currents were calculated using quenched single particle currents, as given above. In the 3.198 MeV state, the currents are dominated by the $\nu(2g_{9/2}, 3p_{1/2}{}^{-1})$ configuration that gives rise to the high Fourier components and causes the dominant transverse cross section on the fourth maximum at $q_{\text{eff}}=2.6$ fm^{-1}. For this state, the small amplitudes of the $\pi(1h_{9/2}, 3s_{1/2}{}^{-1})$, $\nu(1i_{11/2}, 3p_{1/2}{}^{-1})$, and $\nu(2g_{9/2}, 2f_{5/2}{}^{-1})$ components were fitted as well as an effective magnetic moment.

For the 3.709 and 3.961 MeV states, the maximum sensitivity to the transverse current is around the second maximum in the form factor where the transverse cross section from the $\pi(1h_{9/2}\ 3s_{1/2}{}^{-1})$ component dominates. These states present an interesting case, since in the rather large transverse electric currents, the convection current from the proton $\pi(1h_{9/2}, 3s_{1/2}{}^{-1})$ configuration gives a strong contribution. Recently, many states have been observed in electron scattering where the transition currents are reduced to about 70% or less of the single particle values.[10,11,30] In all those cases, the currents were produced exclusively by the magnetic moment of the nucleons. Thus, the observed currents in these 5^- levels present the first case known to us where one can get information about the quenching in the convection currents.

The level most sensitive to the proton configuration is obviously the 3.961 MeV state. The fit to our data in which we fit the magnetic quenching f_m separately from the quenching of the convection current f_c gives:

$$f_m=0.43\pm0.015$$

and

$$f_c=0.97\pm0.055\ .$$

Thus, it indicates that in these transitions, only the magnetization current is quenched while the convection current is essentially unquenched.

If we assume that the origin of the observed quenching here is the same as for the quenching observed in the high spin states, this result allows us to distinguish between the model developed by Krewald and Speth[31] and that developed by Hamamoto *et al.*[32,33] In the calculations of Krewald and Speth, the quenching is dominantly caused by fractionation of the strength through mixing with 2p2h configurations. If this interpretation were also applicable for the 5^- states, the magnetization current and the convection current term should be quenched by the same amount. However, if as Hamamoto *et al.* assume, the quenching is caused through core polarization through the residual interaction, the quenching would mainly affect the

magnetization or spin current but not the convection current. Thus, our results seem to favor the interpretation of Hamamoto *et al.*

The transition charge density of the 3.198 MeV and the 3.709 MeV states are defined well enough from our data to warrant a Fourier Bessel Analysis (FBA), as described in Ref. 17. The data for these states include forward scattering data from Mainz[6,8] and some recent data taken at Saclay.[9] These data from Saclay cover the momentum transfer range from $1.25 < q < 3.4$ fm^{-1} and allow a substantial reduction of the incompleteness error. Similar to the observations on the 3^- level at 2.615 MeV,[5] the cross section does not follow a regular diffraction pattern but beyond the momentum transfer of about 2.6 fm^{-1}, drops much faster, showing the lack of high Fourier components in the wave function. It is that feature which justifies the method of estimating the incompleteness error as described in Ref. 17.

For the fitting, we used an iterative procedure: First the 90° data were fit in the FBA. We then fit the 160° data keeping the transition charge density constant and fitting only the current $J^{tr}(r)$ according to the microscopic models, as quoted. The 90° data were then corrected for any contribution from $J^{tr}(r)$ and a new FBA fit was performed, assuming the absence of the current $J^{tr}(r)$. This procedure was repeated until convergence. It represents a separation of longitudinal and transverse form factors in the presence of strong Coulomb distortions.

Since the transition charge of the 3.961 MeV state is not determined as well, we took a more restrictive model to fit the data. The transition charge was composed from an induced charge, which we assumed to have a radial shape similar to the shape of the transition charge observed in the 3.198 MeV state and the $\pi(1h_{9/2}\ 3s_{1/2}{}^{-1})$ ph component calculated from a Woods Saxon well. The current density $J^{tr}(r)$ was composed from single particle densities, as given by the expressions of Eq. (3). Thus, in the determination of the transition charge, only 3 amplitudes were fitted.

The resulting fits to the 90° and 160° are shown in Figs. 6 and 7. The transition charge distributions for the three 5^- states are displayed in Fig. 8.[34] They show the general features described above where for the two lower states, the density peaks at the nuclear surface, while for the transition to the 3.961 MeV 5^- state, the density at the nuclear surface is very small and the main peak of the density is located in the nuclear interior.

In Fig. 8, we compare the experimental results of

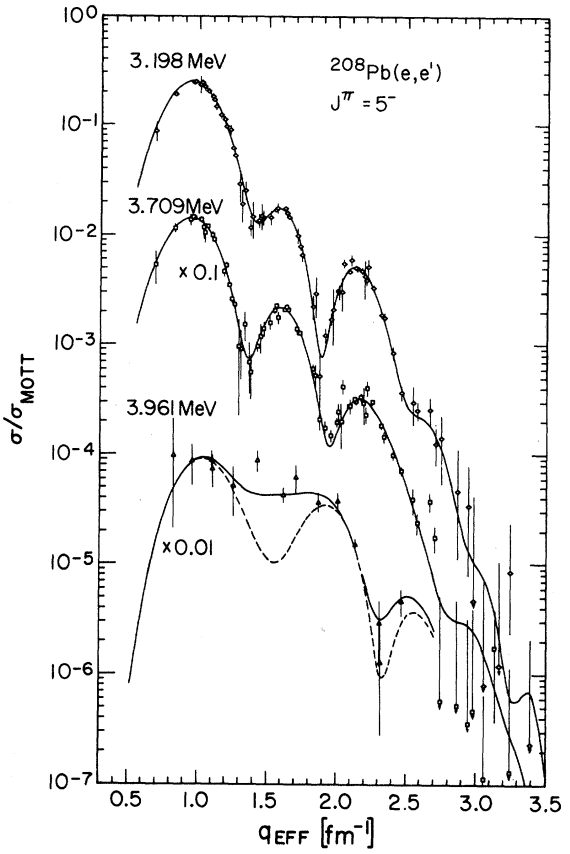

FIG. 6. Cross sections and best fit (divided by σ_M) for the first three 5^- levels in ^{208}Pb for the forward scattering data. The dashed line for the 3.961 MeV level indicates the calculated cross sections without the transverse part. For this level, all data shown were taken at 90°. The data and best fit for the 3.709 MeV level are scaled down a factor of 0.1, those of the 3.961 MeV level are scaled down a factor of 0.01.

the 3.198 MeV and the 3.709 MeV level to some theoretical calculations of different degrees of sophistication. Curve (b) due to Gogny[35] is the product of a fully self-consistent calculation in which the collective excitations are calculated in the framework of the RPA with the same effective interaction ($D1$) that generated the Hartree-Fock-Bogoliubov basis. The calculation (d) by Bertsch and Tsai[21] is also fully self-consistent based on the zero-range Skyrme interaction, but does not include the pairing aspect. The calculation [curve (a)] by Heisenberg and Krewald,[23] uses the zero-range density dependent interaction similar to that of Speth *et al.*[36] with a ph basis and a parametrization of the residual interaction identical to those used by Rink-

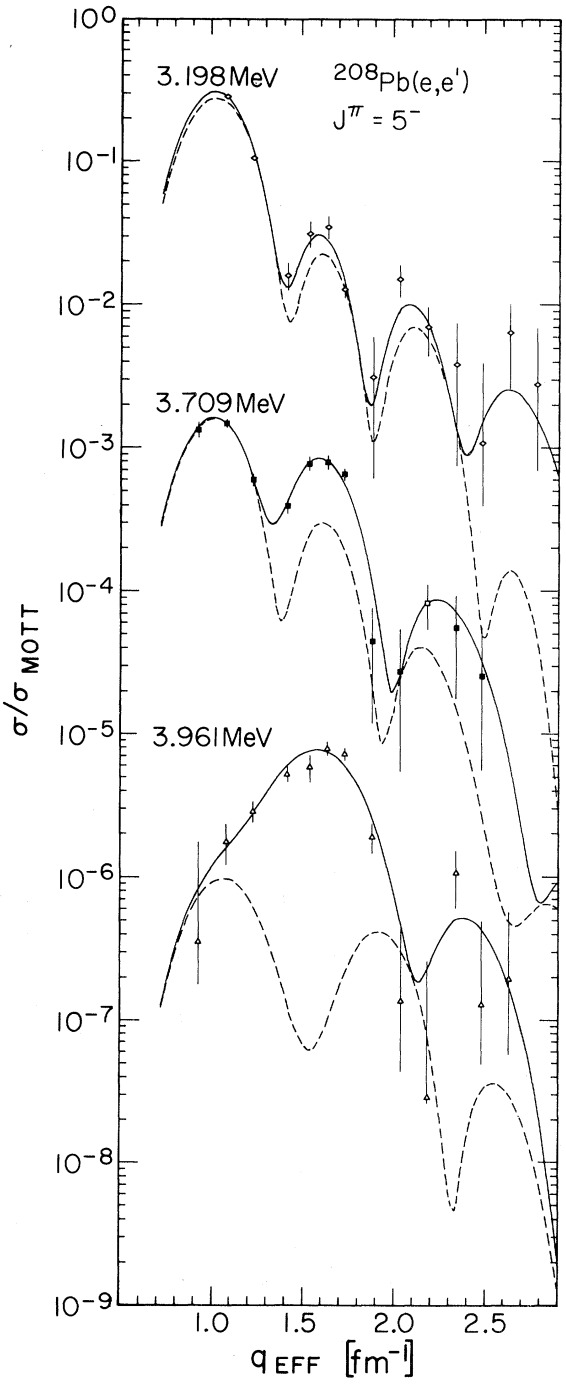

FIG. 7. Cross section and best fit (divided by σ_M) for the backward scattering data of the first three 5^- levels taken at 160°. The dashed line represents the cross section without the transverse current. The deviation of the data from this line gives the sensitivity of the transverse current to the data in the various regions of the momentum transfer. The data of the 3.709 MeV level are scaled down a factor of 0.1, those of the 3.961 MeV level are scaled down a factor of 0.01.

er and Speth.[37] Curve (c) is due to Knüpfer and Huber.[22]

Compared to the generally good agreement obtained for the 3^- level, the agreement for the 5^- levels is poor. While both calculations shown for the 3.709 MeV state give about the correct strength, almost all calculations overpredict the transition charge density at the nuclear surface considerably, even though the $B(E5)$ values are not in strong disagreement with the experimental result. The main cause for this situation is that these states are much less collective. As a consequence, the particle hole energies become very important in determining the relative amplitudes of the various ph components, while in the case of the 3^- level, the physical state is far removed in energy from the ph energies and thus only moderately affected by it. This is particularly visible in the density due to Bertsch and Tsai, which has even the incorrect phasing in the interior structure. This seems to be a general problem of a fully self-consistent approach, since generally one cannot expect that the ph energies are reproduced with the needed precision.

For that reason, one expects those calculations that use experimental ph energies from neighboring odd-even nuclei to give better agreement than the fully self-consistent calculations, especially for the less collective states. However, even the experimental particle and hole energies do not represent the proper Hartree-Fock energies in ^{208}Pb. This becomes particularly apparent in the 3.961 MeV 5^- state where considerable improvement in the description of this state was achieved by reducing the ph energy of the $\pi(1h_{9/2}, 3s_{1/2}{}^{-1})$ component relative to that of the $\nu(2g_{9/2}\ 2f_{5/2}{}^{-1})$ configuration. This reduction was also required to reproduce the experimental excitation energies of the 6^- levels.[38] Thus, the success in describing this transition charge density confirms the need to shift the effective ph energy.

Figure 8 also shows extracted current densities $J^{tr}(r)$. Even though these current densities were not derived in a "model independent" way, they represent the observed currents over the full range of the momentum transfers covered by this experiment. For example, the high frequency of the transition current density of the 3.198 MeV state is not only a requirement of the model but also demanded by the data that show the dominant effect from the transverse current at $q=2.6$ fm^{-1}. The theoretical current densities shown are from Heisenberg and Krewald[23] and strongly overpredict the measured currents except for the 3.709 MeV state.

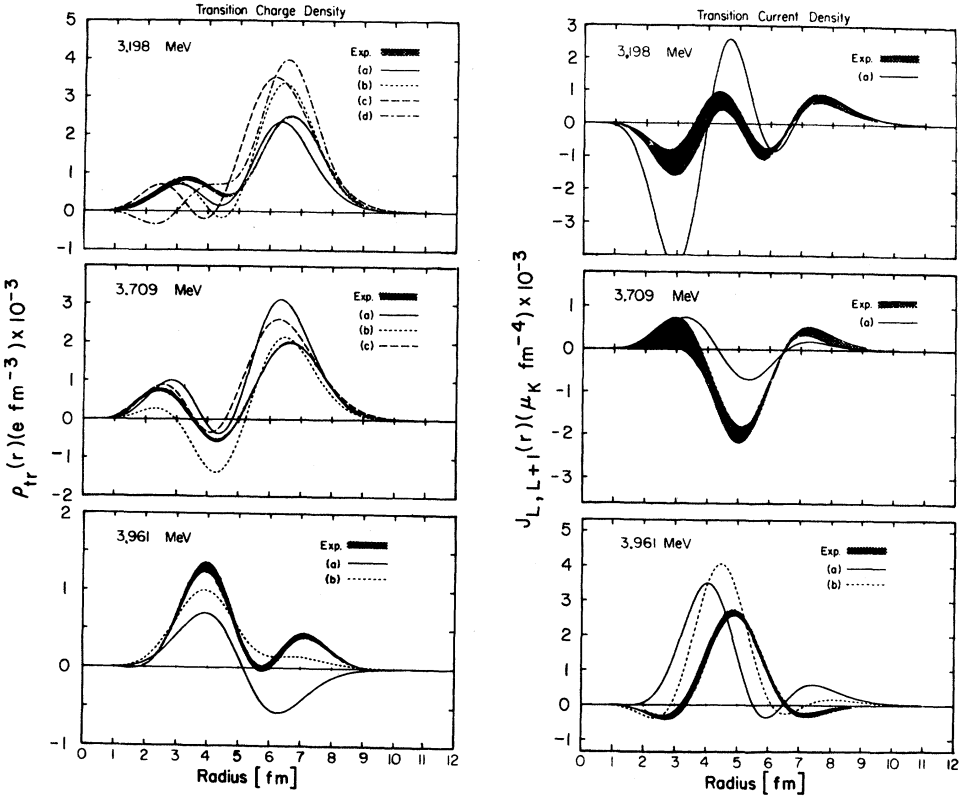

FIG. 8. Transition charge and current densities for the first three 5^- levels in ^{208}Pb. The theoretical curves are (a) from Heisenberg and Krewald (Ref. 23), (b) from Gogny (Ref. 35), (c) from Knüpfer and Huber (Ref. 22), and (d) from Bertsch and Tsai (Ref. 21). For the 3.961 MeV state curves (b) are from Ref. 23 also but calculated with a shifted $h_{9/2}$ energy.

C. The 7^- state at 4.037 MeV

The 7^- state at 4.037 MeV is the lowest state of this multipolarity. Nevertheless, it shows no sign of collectivity. The form factor is dominated by the transverse scattering. This behavior is consistent with the main configuration of the state being a $\nu(2g_{9/2}\ 2f_{5/2}{}^{-1})$ configuration where all the charge scattering is due to the induced charge of the neutron. This charge is small and our data are not very sensitive to the shape of the transition charge density. Because of this lack of sensitivity, the fitting was modified for this state. For the transition charge density, we assumed the identical radial shape of the lowest 7^- excitation at 2.2 MeV in ^{206}Pb, which had been analyzed with the FBA.[17] The magnitude of this transition charge was fit to the data. The transverse currents were described by the model of quenched single particle densities. The single particle wave functions were calculated from a Woods Saxon well with a radius fitted to the data.

Since all the currents originate from the magnetic moment of the neutron, there is no ambiguity as to whether the quenching in the convection current term and in the magnetization current term are the same. A quenching factor $f_m = 0.505$ resulted from the fit.

As can be seen in Fig. 9, fitting the three parameters specified to the data gives quite satisfactory results and measures the spatial extent of this ph configuration. It also shows that similar to the high spin states,[10,11] only about 25% of the predicted single particle strength is observed in the transverse scattering. The induced charge density at the nuclear surface is about 50% of the neutron single particle transition density, equivalent to an "effective charge" of 0.5, again confirming that this is not a collective state.

Figure 10 shows the transition charge and current densities for this state. It should be emphasized that the error bands shown here are strongly model dependent. Considering this, the comparison to the calculations of Ref. 23 show fair agreement in the transition charge even though too much strength is predicted. The transition current is overpredicted

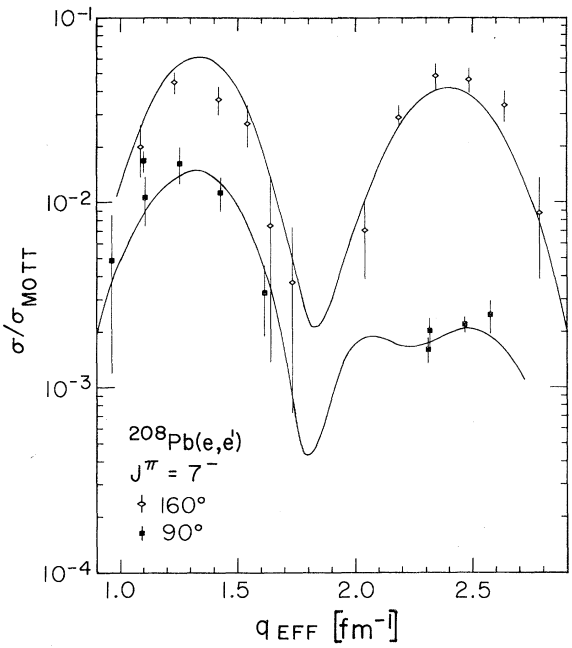

FIG. 9. Cross sections and best fit for the 4.037 MeV 7^- level (divided by σ_M). The upper curve represents data at 160°, the lower curve those taken at 90°.

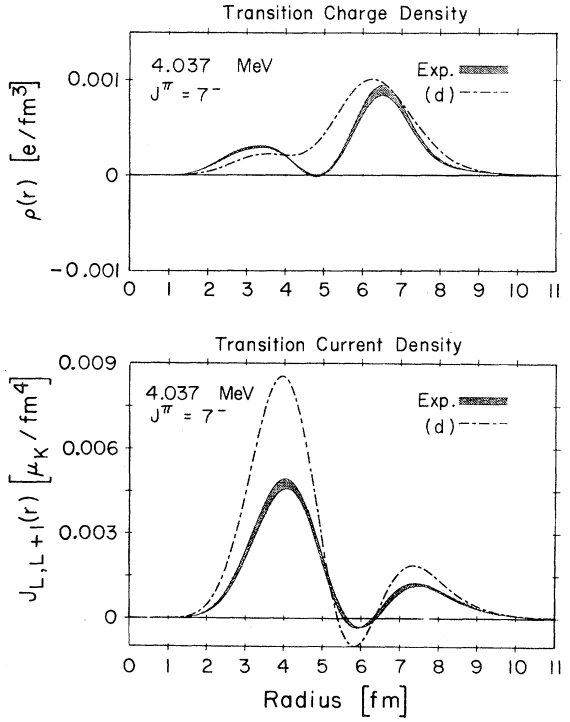

FIG. 10. Transition charge and current density for the 7^- level at 4.037 MeV. The curves are from Heisenberg and Krewald (Ref. 23).

by about a factor of 2.

Table I summarizes the best fit Fourier Bessel coefficients for all the transition charge densities determined. This table also includes the resulting $B(E\lambda)$ values with their statistical uncertainties. It should be noted that this transition probability is, for most levels, an extrapolated quantity and does not represent the best information available from the experiment. The most precise information is usually given through the amplitude of the density at the first maximum.

VII. CONCLUSION

For the positive parity states and the 3^- level, very little transverse electric excitation is observed. That means that the transitions behave like irrotational, incompressible flow as described by the modified Tassie model. Transition charge densities have been extracted for these transitions and compared to various RPA calculations. The theoretical predictions for these transition charge densities give generally the proper shapes dominated by the surface peaked nature. Nevertheless, large discrepancies remain in such details as the magnitude of the interior structures and the overall strength of the transition.

For the negative parity electric transitions as well as for the positive parity states, we observe a drastic decrease in collectivity with increasing multipolarity. This result is consistent with results from other probes and seems to justify the interpretation of the high spin states as dominantly individual 1p1h configurations. This reduction in strength for the high multipolarities comes to some extent from the density of states in the basis. It also depends strongly on the proper q dependence or L dependence of the residual interaction. Our data, with those results given in Ref. 11, span the range $\lambda=2$ to $\lambda=12$ in multipolarity, corresponding to the momentum transfer range as given by the first and dominant maximum in the form factor of 0.5 to 2.1 fm^{-1}. Thus, these data seem to be particularly suited to check the effective q dependence of the residual interaction in any theoretical calculation.

The negative parity states show significant transverse form factors. In all cases, the transverse strength is quenched to about at least 50% of the single particle strength. There seems to be an indication in our data that only the contribution from the magnetization current is quenched while the convection current contribution is unquenched. This quenching of the magnetization contribution has manifested itself in a wide range of transitions

of different multipolarities and regions of the Periodic Table.[39] Similar effects have been observed in other reactions, most notably in the excitation of the Gamow Teller resonances.[40] Our results imply that the mechanism for the quenching is not caused by fractionation or through correlations in the ground state, but either through a residual spin exchange interaction or through meson exchange corrections.[41]

The interpretation of the currents in terms of single particle transition currents including only a few components should be used with caution if these amplitudes are interpreted to represent the spectroscopic factors for these configurations in the observed state, since it implies that the quenching in the ph components is independent of the configuration and excitation energy and can be represented through an effective magnetic moment. On the other hand, one may treat it as just a convenient parametrization of the transition current, which, once it describes the observed cross sections in the range of the momentum transfer of the data, supplies a proper representation of the nuclear current density.

The presented results show a great variety of phenomena: collective surface peaked densities, almost pure single particle states, or states where the transition charge density lies in the interior of the nucleus. The theoretical RPA predictions of these transitions are very sensitive to the ph energies. Thus, in a completely self-consistent treatment, it is impossible to reproduce all these observed features. With readjusted ph energies, the densities are very sensitive measures of the details of the residual interaction such as the density dependence, the nonlocality, and the spin or isospin exchange admixtures.

The results presented are part of a more general investigation[42,43] of the stable Pb isotopes. Infortion on many more excited states has been obtained, which will be subject to further publications. All data or listings of densities can be obtained from the authors.

This work was supported in part by the U. S. Department of Energy Contract No. DE-AS02-ER10338.

[1]B. Frois, J. B. Bellicard, J. M. Cavedon, M. Huet, P. Leconte, P. Ludeau, A. Nakada, Phan Xuan Ho, and I. Sick, Phys. Rev. Lett. 38, 152 (1977).

[2]J. L. Friar, J. W. Negele, and J. Heisenberg, in Proceedings of the June Workshop in Intermediate Energy Electromagnetic Interactions with Nuclei, edited by A. M. Bernstein, Massachusetts Institute of Technology (MIT), 1977 (unpublished).

[3]J. L. Friar and J. W. Negele, *Advances in Nuclear Physics* (Plenum, New York, 1975), Vol. 8, p. 219.

[4]J. Dechargé and D. Gogny, Phys. Rev. C 21, 1568 (1980).

[5]D. Goutte, J. B. Bellicard, J. M. Cavedon, B. Frois, M. Huet, P. Leconte, Phan Xuan Ho, S. Platchkov, J. Heisenberg, J. Lichtenstadt, C. N. Papanicolas, and I. Sick, Phys. Rev. Lett. 45, 1618 (1980).

[6]J. Friedrich, Nucl. Phys. A191, 118 (1972).

[7]M. Nagao and Y. Torizuka, Phys. Lett. 37B, 383 (1971); and K. Arita and T. Teresawa, in *Proceedings of the International Conference on Studies Using Electron Scattering and Photoreactions, Sendai, Japan, 1972,* edited by K. Shoda and H. Ui (Tohoku University, Sendai, 1972).

[8]J. Friedrich, N. Voegler, and H. Euteneuer, Phys. Lett. 64B, 269 (1976).

[9]C. N. Papanicolas, J. Heisenberg, J. Lichtenstadt, J. S. McCarthy, D. Goutte, J. M. Cavedon, B. Frois, M. Huet, P. Leconte, Phan Xuan Ho, S. Platchkov, and I. Sick, Phys. Lett. 108B, 279 (1982).

[10]J. Lichtenstadt, J. Heisenberg, C. N. Papanicolas, C. P. Sargent, A. N. Courtemanche, and J. S. McCarthy, Phys. Rev. C 20, 497 (1979).

[11]J. Lichtenstadt, C. N. Papanicolas, C. P. Sargent, J. Heisenberg, and J. S. McCarthy, Phys. Rev. Lett. 44, 858 (1980).

[12]W. Bertozzi, M. V. Hynes, C. P. Sargent, C. Creswell, P. C. Dunn, A. Hirsch, M. Leitch, B. Norum, F. N. Rad, and T. Sasanuma, Nucl. Instrum. Methods 141, 457 (1977).

[13]W. Bertozzi, M. V. Hynes, C. P. Sargent, W. Turchinetz, and C. Williamson, Nucl. Instrum. Methods 162, 211 (1979).

[14]P. C. Dunn, Nucl. Instrum. Methods 165, 163 (1979).

[15]J. Bergstrom, in Medium Energy Nuclear Physics, Massachusetts Institute of Technology (MIT), 1967, Summer Study, edited by W. Bertozzi and S. Kowalski MIT, 1967 (unpublished), p. 251.

[16]W. T. Wagner, C. M. Crawley, G. R. Hammerstein, and H. McManus, Phys. Rev. C 12, 757 (1975).

[17]J. Heisenberg, *Advances in Nuclear Physics,* edited by J. Negele and E. Vogt (Plenum, New York, 1981), Vol. 12, p. 61.

[18]H. C. Lee, Nuclear Charge, Convection Current, and Magnetization Current Densities, Atomic Energy Commission Laboratory, Report AECL 4839, 1975 (unpublished).

[19]L. J. Tassie, Aust. J. Phys. 9, 407 (1956).
[20]J. P. Ziegler and G. A. Peterson, Phys. Rev. 165, 1337 (1968).
[21]G. F. Bertsch and S. F. Tsai, Phys. Rep. 18, 125 (1975); and private communication.
[22]W. Knüpfer and M. G. Huber, Phys. Rev. C 14, 2254 (1976); and private communication.
[23]J. Heisenberg and S. Krewald (unpublished).
[24]J. Heisenberg and I. Sick, Phys. Lett. B32, 249 (1970).
[25]H. Rothhaas, J. Friedrich, K. Merle, and B. Dreher, Phys. Lett. B51, 23 (1974).
[26]P. B. Vold, J. O. Andreassen, J. R. Lien, A. Graue, E. R. Cosman, W. Dunnweber, D. Schmitt, and F. Nusslin, Nucl. Phys. A215, 61 (1973).
[27]E. A. McClatchie, C. Glashausser, and D. L. Hendrie, Phys. Rev. C 1, 1828 (1970).
[28]C. N. Papanicolas, J. Heisenberg, J. Lichtenstadt, A. N. Courtemanche, and J. S. McCarthy, Phys. Rev. Lett. 41, 537 (1978).
[29]A. Heusler and P. von Brentano, Ann. Phys. (N. Y.) 75, 381 (1973).
[30]C. N. Papanicolas, J. Lichtenstadt, C. P. Sargent, J. Heisenberg, and J. S. McCarthy, Phys. Rev. Lett. 45, 106 (1980).
[31]S. Krewald and J. Speth, Phys. Rev. Lett. 45, 417 (1980).
[32]I. Hamamoto, J. Lichtenstadt, and G. F. Bertsch, Phys. Lett. B93, 213 (1980).
[33]I. Hamamoto, J. Lichtenstadt, and G. F. Bertsch, Phys. Lett. B96, 249 (1980).
[34]The transition charge densities for the 3.198 MeV and the 3.709 MeV states are identical with the ones from Ref. 9 and are shown here for completeness.
[35]D. Gogny, in *Lecture Notes in Physics,* edited by H. Arenhövel and D. Drechsel (Springer, Berlin, 1979), Vol. 108; and private communication; J. P. Blaizot and D. Gogny, Nucl. Phys. A284, 429 (1977).
[36]J. Speth, E. Werner, and W. Wild, Phys. Rep. 33, 127 (1977).
[37]G. A. Rinker and J. Speth, Nucl. Phys. A306, 360 (1978).
[38]J. Lichtenstadt, J. Heisenberg, C. N. Papanicolas, J. S. McCarthy, and S. Krewald (unpublished).
[39]W. Steffen, H. D. Graff, W. Gross, D. Meuer, A. Richter, E. Spamer, O. Titze, and W. Knüpfer, Phys. Lett. B95, 23 (1980).
[40]C. D. Goodman, Comm. Nucl. Part. Phys. 10, 117 (1981).
[41]A. Bohr and B. Mottelson, Phys. Lett. B100, 10 (1981).
[42]J. Lichtenstadt, Ph.D. thesis, Massachusetts Institute of Technology (MIT), 1979 (unpublished).
[43]C. N. Papanicolas, Ph.D. thesis, Massachusetts Institute of Technology (MIT), 1979 (unpublished).